Cosmological Implications of the GWTC-3 Modified-Propagation Anomaly: Inference Bias in the Hubble Tension

Aiden B. Smith
Independent Researcher
(Dated: February 10, 2026)

We investigate cosmological implications of the GWTC-3 O3 modified-propagation anomaly using an updated Planck-facing calibration chain. The upstream anomaly repository is archived on Zenodo (DOI: 10.5281/zenodo.18585598). A 60-restart Planck+MG global refit defines a revised sound-horizon calibration anchor, $H_0^{\rm Planck,MG} \approx 68.0$, $\Omega_m^{\rm Planck,MG} \approx 0.306$, and $A_{\rm lens} \approx 1.04$ (posterior medians).

The leading result is inference bias: if a modified-gravity truth is analyzed with standard GR sound-horizon compression (standard-ruler inversion), recovered H_0 shifts by mean $\Delta H_0 = +1.88$ km s^{-1} Mpc^{-1} (fixed Ω_m) or $+4.55$ km s^{-1} Mpc^{-1} (lensing-proxy Ω_m), i.e. typical net displacements of order $+2$ to $+5$ km s^{-1} Mpc^{-1} relative to posterior truth.

By contrast, the direct late-time friction channel alone provides limited closure: after rebasing constrained transfer sweeps, the anchor-relief posterior is $\mathcal{R}_{\rm anchor}^{\rm GR} = 0.1545$ (mean; p16/p50/p84 $= 0.108/0.147/0.189$), about 15% of the local-versus-Planck baseline gap.

For CMB lensing, baseline CAMB propagation predicts suppressed power at $L\sim100$ and $L\sim300$ (-15.29% and -9.49% medians). An MG-aware response refit then reaches near-reference quality (median $\chi^2 = 8.06$ vs Planck-reference 9.04). If that additional response freedom is disallowed, the baseline projection remains in strong tension with Planck lensing.

I. SCOPE AND FRAMING

This work treats the O3 modified-propagation signal phenomenologically: given the inferred posterior, what cosmological consequences follow? The O3 anomaly analysis and data products are archived on Zenodo [1]. We do not re-argue detection significance in this manuscript.

Modified GW propagation has been explored in theory-forward frameworks [15, 16]. In this follow-up, we assume the running effective Planck mass $M_\star(z)$ associated with GW friction is a universal MG sector ingredient, so the same $M_\star(z)$ trajectory also modifies the background/scalar channels probed by CMB compression and lensing [17, 18]. Here, we use a data-driven posterior and update the pipeline to answer three questions in one chain:

1. How much late-time Hubble tension relief remains after recalibrating the sound-horizon calibration anchor?

2. Does Planck 2018 lensing necessarily reject this posterior, or can an MG-aware refit absorb the suppression?

3. How much can GR-based standard-ruler inversion bias inferred H_0 if MG truth is assumed?

II. PIPELINE SUMMARY

Posterior draws are taken from `outputs/finalization/highpower_multistart_v2/M0_start101` and propagated through four linked stages:

1. **Global Planck+MG recalibration:** 60-restart multistart fit (`cpuset 0-59`) to establish updated sound-horizon calibration anchor values.

2. **Late-time rebasing:** constrained/pilot transfer sweeps are rebased to the updated Planck-like anchor and recompressed into a final relief posterior.

3. **CMB lensing forecasts:** baseline draw-level CAMB projection to Planck 2018 lensing bandpowers, followed by an MG-aware two-parameter lensing refit.

4. **Compressed standard-ruler inversion:** GR inversion of $\theta_\star = r_d/D_M(z_\star)$ under fixed-Ω_m and lensing-proxy-Ω_m assumptions.

These are targeted forecasts and refits, not a full MG TT/TE/EE perturbation-sector likelihood analysis.

III. RESULTS

A. Updated sound-horizon calibration anchor from the global Planck+MG fit

The 60-restart Planck+MG run completed all restarts with 5 converged minima and 55 max-evaluation exits. Using converged minima only, we obtain:

$$H_0^{\rm Planck,MG} = 68.005302\ (\text{p50}), \quad \Omega_m^{\rm Planck,MG} = 0.30643039\ (\text{p50}), \quad (1)$$

With local reference $H_0^{\rm local} = 73.0$, the baseline gap used in rebased relief calculations is

$$\Delta H_0^{\rm base} = \left| H_0^{\rm local} - H_0^{\rm Planck,MG} \right| = 4.994698. \quad (2)$$

B. Inference bias from GR standard-ruler inversion

To isolate model-assumption bias, we treat MG posterior draws as truth and invert $\theta_\star = r_d/D_M(z_\star)$ with a GR compression model:

- fixed $\Omega_m = \Omega_m^{\rm Planck,MG}$: $H_{0,\rm inferred}$ mean 72.394 (p50 73.170), with mean $\Delta H_0 = +1.876$ km s^{-1} Mpc^{-1} relative to draw-level truth;
- lensing-proxy Ω_m: $H_{0,\rm inferred}$ mean 75.065 (p50 75.226), with mean $\Delta H_0 = +4.547$ km s^{-1} Mpc^{-1}.

The wider lensing-proxy interval reflects the expected H_0–Ω_m degeneracy once the artificial rigidity of the ΛCDM standard ruler is removed; in this channel, the analysis releases model-imposed precision rather than exhibiting numerical instability.

Relative to the recalibrated Planck+MG anchor $H_0^{\rm Planck,MG} = 68.005$, the posterior medians shift by:

$$\Delta H_0^{\rm truth} \approx +2.39, \quad \Delta H_0^{\rm fixed\ inversion} \approx +5.16, \quad \Delta H_0^{\rm lensing\ inversion} \approx +7.22\ \text{km s}^{-1}\ \text{Mpc}^{-1} \tag{3}$$

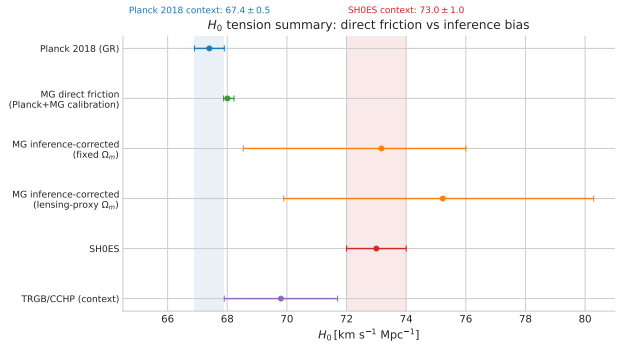

FIG. 1. H_0 tension summary comparing Planck 2018 (GR), direct-friction recalibration, two GR-inversion bias channels, and local-distance-ladder context (SH0ES and TRGB/CCHP [5, 6]). The dominant displacement comes from GR standard-ruler inversion bias when MG truth is assumed; the broad lensing-proxy interval is the expected H_0–Ω_m degeneracy once the artificial ΛCDM standard-ruler rigidity is relaxed.

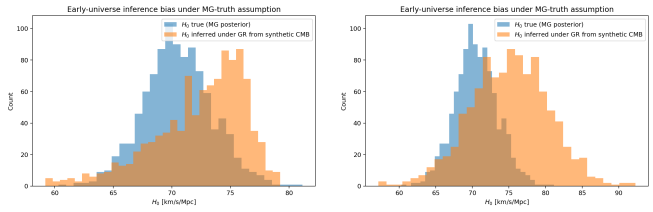

FIG. 2. Draw-level H_0 truth versus GR-inferred H_0 under compressed standard-ruler inversion with fixed-Ω_m (left) and lensing-proxy-Ω_m (right). Both assumptions bias inferred H_0 upward, with larger displacement in the lensing-proxy case.

C. Direct friction channel after late-time rebasing

After rebasing constrained transfer sweeps to the updated sound-horizon calibration anchor and applying Monte Carlo calibration:

$$\mathcal{R}_{\rm anchor}^{\rm GR} = 0.1545 \quad \text{(mean; p16/p50/p84 } = 0.1085/0.1475/0.1891\text{)}. \tag{4}$$

Independent robustness and joint-fit diagnostics are:

- 10-case robustness grid: posterior-shift relief mean 0.5296 (p50 0.5125, p84 0.5453), with zero failed cases.
- Joint SN+BAO+CC transfer fit: relief posterior mean 0.8329 (p50 0.8386), but

$$\log \text{BF}_{\rm transfer/no\text{-}transfer} = -0.533, \tag{5}$$

  so explicit transfer terms are not favored in this setup.

The high-z transfer-bias sensitivity map used for calibration has been moved to supplemental material (Fig. S1).

D. CMB lensing: baseline suppression and MG-aware response freedom

Baseline draw-level CAMB projection against Planck 2018 lensing bandpowers (`consext8`, 64 draws) gives:

$$\left.\frac{C_L^{\phi\phi}(\text{MG})}{C_L^{\phi\phi}(\text{Planck ref})}\right|_{L\approx 106} = 0.847^{+0.091}_{-0.127}, \tag{6}$$

$$\left.\frac{C_L^{\phi\phi}(\text{MG})}{C_L^{\phi\phi}(\text{Planck ref})}\right|_{L\approx 286} = 0.905^{+0.068}_{-0.080}, \tag{7}$$

with median suppressions of −15.29% and −9.49%. The baseline fit quality is poor relative to the Planck-reference model:

$$\chi^2_{\rm MG,baseline}\ \text{(median)} = 51.77, \qquad \chi^2_{\rm Planck\ ref} = 9.04, \tag{8}$$

and only 3.1% of draws outperform the reference. A 32-draw cross-check from an independent posterior sample is more discrepant (−18.66% at $L \approx 106$, −11.29% at $L \approx 286$; $p_{\rm better} = 0$).

To test whether this baseline mismatch is rigid, we perform an MG-aware lensing refit (32 draws) with a phenomenological effective-$M_\star^2$ amplitude plus ℓ-tilt response. This freedom is motivated by scalar-tensor/EFT treatments where matter-growth and light-deflection responses need not track identically and can acquire scale dependence [17, 18]. The refit removes the baseline mismatch:

$$\chi^2_{\rm MG\ refit}\ \text{(median)} = 8.06, \tag{9}$$

better than the Planck-reference $\chi^2 = 9.04$ in 100% of refit draws. This refit is phenomenological and demonstrates model-class freedom, not a unique derivation of one covariant MG Lagrangian. The fitted median response corresponds to

$$\frac{M_\star^2(z=0)}{M_\star^2(z\gg 1)} \simeq 0.901 \tag{10}$$

(about a 9.9% drop), with small residual suppression at $L \approx 286$.

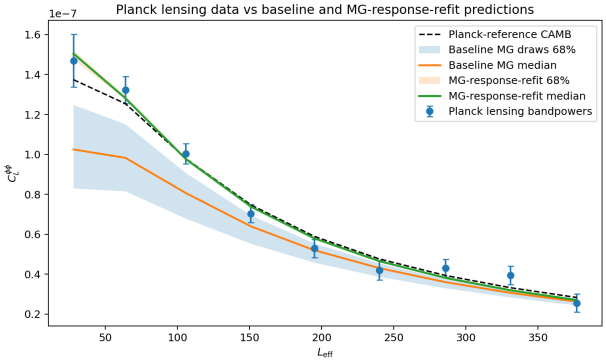

FIG. 3. Planck 2018 lensing bandpowers with baseline MG projection and MG-aware refit overlay. The refit absorbs the baseline suppression and restores near-reference fit quality.

IV. DISCUSSION AND CONCLUSION

The main implication is that inference bias from GR-assumed standard-ruler inversion can be cosmologically large if the O3 modified-propagation posterior corresponds to physical MG truth. In this pipeline, that channel displaces recovered H_0 by order +2 to +5 km s^{-1} Mpc^{-1} relative to draw-level truth, with larger shifts relative to the recalibrated Planck+MG anchor.

The direct friction channel remains subdominant in the constrained rebased analysis: $\mathcal{R}^{\rm GR}_{\rm anchor} \simeq 0.15$. This means the principal lever in this study is model-assumption bias from GR-assumed standard-ruler inversion, not direct late-time closure alone.

For CMB lensing, baseline propagation is strongly discrepant with Planck 2018. An MG-aware response refit motivated by effective-coupling freedom in scalar-tensor/EFT descriptions restores near-reference likelihood performance. If that response freedom is not permitted, the baseline projection remains in strong tension with lensing data.

Taken together, these results recast the follow-up question from "does friction alone close the full tension?" to "how much of the inferred early-versus-late mismatch can come from GR-compression bias when MG truth is present?" In this analysis, that range is material and should be included in future MG-aware CMB-to-late-time consistency tests.

REPRODUCIBILITY

Core scripts used in this follow-up are:

- `scripts/run_planck_global_mg_refit_multistart.py`
- `scripts/rebase_bias_transfer_sweep_to_planck_ref.py`
- `scripts/run_hubble_tension_final_relief_posterior.py`
- `scripts/run_hubble_tension_mg_forecast_robustness_grid.py`
- `scripts/run_joint_transfer_bias_fit.py`
- `scripts/run_hubble_tension_cmb_forecast.py`
- `scripts/run_hubble_tension_mg_lensing_refit.py`
- `scripts/run_hubble_tension_early_universe_bias.py`

ACKNOWLEDGMENTS

This work used A.I. tools extensively, including ChatGPT 5.3.

DATA AVAILABILITY AND DOIS

The follow-up uses posterior products from the O3 anomaly pipeline and public cosmology datasets. Data provenance and DOIs are:

- O3 modified-gravity tension anomaly repository (Zenodo): DOI 10.5281/zenodo.18585598.
- O3 search-sensitivity injection data used in upstream calibration (Zenodo): DOI 10.5281/zenodo.7890437.
- GWTC-3 catalog paper: DOI 10.1103/PhysRevX.13.041039.
- Pantheon+ cosmology constraints: DOI 10.3847/1538-4357/ac8e04.
- SH0ES local-H_0 reference: DOI 10.3847/2041-8213/ac5c5b.
- TRGB/CCHP local-H_0 context reference: DOI 10.3847/1538-4357/ab2f73.
- SDSS DR12 BOSS consensus BAO (source of `sdss_DR12Consensus_bao.dat`): DOI 10.1093/mnras/stx721.
- eBOSS DR16 cosmological compilation (source class for `sdss_DR16_LRG_BAO_DMDH.dat`): DOI 10.1103/PhysRevD.103.083533.
- DESI 2024 BAO cosmological constraints (source class for `desi_2024_gaussian_bao_ALL_GCcomb_mean.txt`): DOI 10.1088/1475-7516/2025/02/021.
- Cosmic-chronometer compilation components used in `Hz_BC03_all.dat`: DOIs 10.1088/1475-7516/2012/08/006, 10.1103/PhysRevD.71.123001, and 10.1088/1475-7516/2010/02/008.
- Planck 2018 cosmological-parameter and lensing references: DOIs 10.1051/0004-6361/201833910 and 10.1051/0004-6361/201833886.

[1] A. B. Smith, "O3 Modified Gravity Tension Replication," Zenodo (2026), DOI: 10.5281/zenodo.18585598.

[2] LIGO Scientific Collaboration, Virgo Collaboration, and KAGRA Collaboration, "GWTC-3: Compact Binary Coalescences Observed by LIGO and Virgo During the Second Part of the Third Observing Run — O3 search sensitivity estimates," Zenodo (2023), DOI: 10.5281/zenodo.7890437.

[3] R. Abbott *et al.* (LIGO Scientific Collaboration, Virgo Collaboration, and KAGRA Collaboration), "GWTC-3: Compact Binary Coalescences Observed by LIGO and Virgo During the Second Part of the Third Observing Run," *Phys. Rev. X* **13**, 041039 (2023), DOI: 10.1103/PhysRevX.13.041039.

[4] D. Brout *et al.*, "The Pantheon+ Analysis: Cosmological Constraints," *Astrophys. J.* **938**, 110 (2022), DOI: 10.3847/1538-4357/ac8e04.

[5] A. G. Riess *et al.*, "A Comprehensive Measurement of the Local Value of the Hubble Constant with 1 km s^{-1} Mpc^{-1} Uncertainty from the Hubble Space Telescope and the SH0ES Team," *Astrophys. J. Lett.* **934**, L7 (2022), DOI: 10.3847/2041-8213/ac5c5b.

[6] W. L. Freedman *et al.*, "The Carnegie-Chicago Hubble Program. VIII. An independent determination of the Hubble constant based on the tip of the red giant branch," *Astrophys. J.* **882**, 34 (2019), DOI: 10.3847/1538-4357/ab2f73.

[7] S. Alam *et al.*, "The clustering of galaxies in the completed SDSS-III Baryon Oscillation Spectroscopic Survey: cosmological analysis of the DR12 galaxy sample," *Mon. Not. R. Astron. Soc.* **470**, 2617 (2017), DOI: 10.1093/mnras/stx721.

[8] S. Alam *et al.*, "Completed SDSS-IV extended Baryon Oscillation Spectroscopic Survey: Cosmological implications from two decades of spectroscopic surveys at the Apache Point Observatory," *Phys. Rev. D* **103**, 083533 (2021), DOI: 10.1103/PhysRevD.103.083533.

[9] DESI Collaboration, "DESI 2024 VI: cosmological constraints from the measurements of baryon acoustic oscillations," *J. Cosmol. Astropart. Phys.* **02** (2025) 021,

DOI: 10.1088/1475-7516/2025/02/021.

[10] M. Moresco *et al.*, "Improved constraints on the expansion rate of the Universe up to $z \sim 1.1$ from the spectroscopic evolution of cosmic chronometers," *J. Cosmol. Astropart. Phys.* **08** (2012) 006, DOI: 10.1088/1475-7516/2012/08/006.

[11] J. Simon, L. Verde, and R. Jimenez, "Constraints on the redshift dependence of the dark energy potential," *Phys. Rev. D* **71**, 123001 (2005), DOI: 10.1103/PhysRevD.71.123001.

[12] D. Stern *et al.*, "Cosmic chronometers: constraining the equation of state of dark energy. I: $H(z)$ measurements," *J. Cosmol. Astropart. Phys.* **02** (2010) 008, DOI: 10.1088/1475-7516/2010/02/008.

[13] N. Aghanim *et al.* (Planck Collaboration), "Planck 2018 results. VI. Cosmological parameters," *Astron. Astrophys.* **641**, A6 (2020), DOI: 10.1051/0004-6361/201833910.

[14] N. Aghanim *et al.* (Planck Collaboration), "Planck 2018 results. VIII. Gravitational lensing," *Astron. Astrophys.* **641**, A8 (2020), DOI: 10.1051/0004-6361/201833886.

[15] E. Belgacem, Y. Dirian, S. Foffa, and M. Maggiore, "Modified gravitational-wave propagation and standard sirens," *Phys. Rev. D* **98**, 023510 (2018), DOI: 10.1103/PhysRevD.98.023510.

[16] A. Nishizawa, "Generalized framework for testing gravity with gravitational-wave propagation," *Phys. Rev. D* **97**, 104037 (2018), DOI: 10.1103/PhysRevD.97.104037.

[17] E. Bellini and I. Sawicki, "Maximal freedom at minimum cost: linear large-scale structure in general modifications of gravity," *J. Cosmol. Astropart. Phys.* **07** (2014) 050, DOI: 10.1088/1475-7516/2014/07/050.

[18] L. Pogosian and A. Silvestri, "What can cosmology tell us about gravity? Constraining Horndeski gravity with Σ and μ," *Phys. Rev. D* **94**, 104014 (2016), DOI: 10.1103/PhysRevD.94.104014.